Performance Analysis in a PAM-4 Fiber Transmission IM-DD with Pre-compensation Filter

ALESSANDRO VIGANÒ, MAURIZIO MAGARINI, ARNALDO SPALVIERI
Politecnico di Milano
Dipartimento di Elettronica, Informazione e Bioingegneria
Piazza Leonardo da Vinci 32, 20133 Milano
ITALY
arnaldo.spalvieri@polimi.it

Abstract: In this paper we study the performance of 4-ary pulse amplitude modulation (PAM-4) transmission using intensity modulation with direct detection (IM-DD) on a fiber link of 80 km. The system uses a pre-compensation filter to take care of the chromatic dispersion. Specifically, it is studied the effect of the difference between nominal chromatic dispersion used in the pre-compensation filter and the actual value of the chromatic dispersion introduced by the fiber. This is because the actual length of the fiber can be different from the designed one and, also, because the dispersion parameter can vary because of changing in refractive index of the fiber that can be caused by the temperature variation. Simulation results obtained by means of Monte Carlo simulations are used to show the sensitivity of bit error rate performance to the mismatch between nominal and actual value of the chromatic dispersion.

Key–Words: Pulse amplitude modulation (PAM), intensity modulation, direct detection, non-coherent demodulation, chromatic dispersion

1 Introduction

Intensity modulation with direct detection is an attractive technique for short-reach optical systems used in optical access and backhauling, see e.g. [1, 2, 3]. These systems should meet the requirement of low cost and this rules out coherent systems, which need multi-giga sample per second data conversion and complex receivers that counteract fiber impairments, as, e.g., non-linear phase noise [4, 5]. Both multitone modulation [6, 7] and conventional amplitude modulation are candidate modulation schemes. In the following we study four-level pulse amplitude modulation (PAM-4). In intensity modulation (IM) PAM-4 transmission with direct detection (DD), chromatic dispersion must be compensated before detection and, therefore, powerful digital equalization schemes such as [8], cannot be employed at the receive side. Besides optical compensation, what one can do is to pre-compensate for chromatic dispersion at the transmit side with a baseband digital filter [9]. However, for pre-compensation to be effective, one has to know the dispersion parameter and the fiber length, which are known with a limited precision.

In this paper we study the effect of errors due to inexact knowledge of dispersion parameter and fiber length in pre-compensation. To do this, we com-pute the Error Vector Magnitude (EVM) [11] and the Signal-to-Distortion Ratio (SDR) that result from the mismatch between the actual parameters and those used in the design and show that they can be used to get a good approximation to the Bit error Rate (BER).

The paper is organized as follow. In Sec. 2 we introduce the system model. Performance analysis and Monta Carlo simulations are presented in Sec. 3. Finally, conclusions are drawn in Sec. 4.

2 PAM-4 System Model

The baseband equivalent discrete-time model considered for the system studied in the paper is reported in Fig. 1. The input bit stream $\{b_k\}$ is mapped on a PAM-4 constellation by the modulator to generate the sequence of transmitted symbols $\{a_k\}$. Since IM is considered, the amplitudes of the transmitted symbols are only positive, due to the direct detection technique used at the receiver. We assume Gray mapping where transmitted symbols are randomly drawn from the set of equiprobable values $\mathcal{A} = \{1, 3, 5, 7\}$. Always with reference to Fig. 1, $h_P(k)$ denotes the discrete-time impulse response of the pre-compensation filter. The role of $h_P(k)$ is that of compensating for the chromatic dispersion introduced by the channel. The pre-
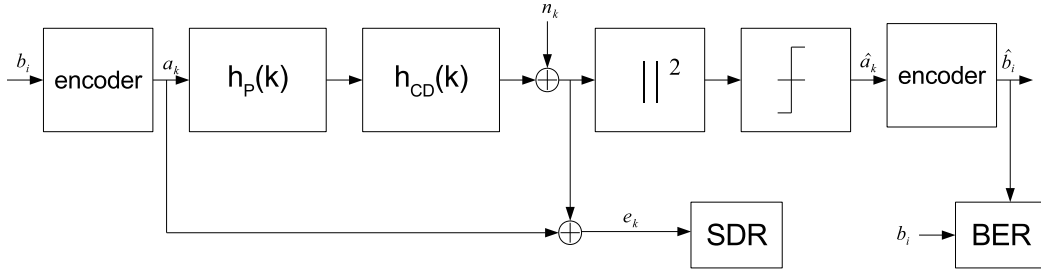
Figure 1: Complete scheme of the system model

compensation filter can be pre-calculated by computing the inverse Fourier Transform of the complex conjugate of the frequency response of the chromatic dispersion, which is given by

$$H_{CD}(f) = \exp(-j\frac{1}{2}\beta_2 f^2 L), \qquad (1)$$

where β_2 denotes the chromatic dispersion parameter, L is the length of the fiber link and f is the frequency.

Often $H_{CD}(f)$ is written as a function of the dispersion parameter D, defined as

$$D = -\frac{f_0^2}{2\pi c}\beta_2$$

where c is the light speed, λ is the carrier wavelength. The measure unit of the dispersion parameter is $[\mathrm{ps}/(\mathrm{nm} \cdot \mathrm{km})]$. By replacing in (1) we get

$$H_{CD}(f) = \exp(\frac{j\pi DL\lambda^2}{c}f^2). \qquad (2)$$

It follows that the continuous-time impulse response of the pre-compensation filter is given by

$$h_P(t) = \mathcal{F}^{-1}\{H_P(f)\} = \mathcal{F}^{-1}\left\{\exp\left(-\frac{j\pi DL\lambda^2}{c}f^2\right)\right\}, \qquad (3)$$

where $\mathcal{F}^{-1}$ is the inverse Fourier transform operator. The discrete-time impulse response $h_P(k)$ is obtained by approximating the computation of inverse Fourier transform with inverse discrete Fourier transform, where a sampling in frequency domain is chosen to avoid aliasing in time-domain. The parameters that are hereafter used to derive numerical results presented in the following are

- $\lambda = 1.54294$ nm

- $D = 16.5$ ps/nm/km

- $L = 80$ km

- $f = 50$ GHz

A discrete-time zero-mean complex white Gaussian noise $\{n_k\}$ with variance σ_n^2 is added to the signal at the input of the photo-detector. After the square law detection operated by the photo-detector, a decision is taken by applying the signal at the input of the memoryless threshold detector. Same transmitted amplitude levels are assumed at the output of the photo-detector without noise. Independent decisions are taken by comparison with equally spaced thresholds centered at the medium distance between constellation points. The estimated symbols $\hat{a}_k$ are then de-mapped by the demodulator and the stream of decided bits $\hat{b}_i$ is output.

The signal before the photo-detector can be represented as

$$r_k = a_k \otimes h_M(k) + n_k, \qquad (4)$$

where $\otimes$ denotes discrete convolution and

$$h_M(k) = h_P(k) \otimes h_{CD}(k). \qquad (5)$$

is the impulse response of the cascade of pre-compensation filter and actual chromatic dispersion channel. In case of ideal pre-compensation, $h_M(k)$ results in a ideal Kronecker delta

$$\delta_k = \begin{cases} 1, & k = 0, \\ 0, & k \neq 0. \end{cases}$$

However, in presence of mismatch, $h_M(k)$ broadens its temporal duration and Inter Symbol Interference (ISI) arises. This means that the received symbol is overlapped with the tails of the impulse response of the previous symbols and this creates distortion that finally results in performance degradation. In the Section that follows different Figure of merits are adopted to evaluate the entity of this performance degradation.

3 Performance Analysis

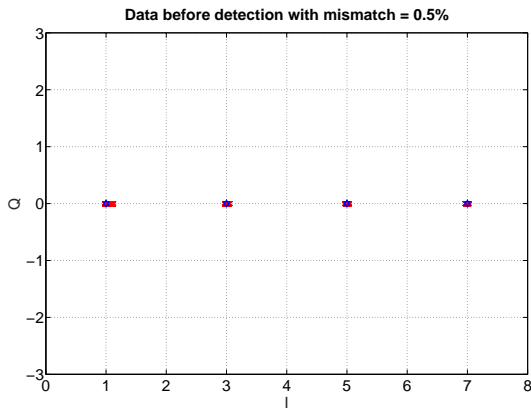With the help of a simulation, these types of analysis have been done:

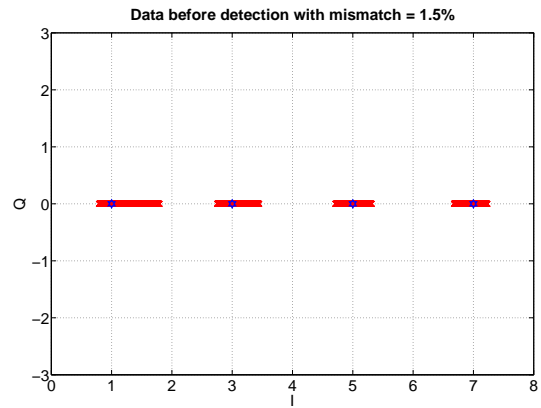Figure 2: Scatter plot with 0.5% mismatch

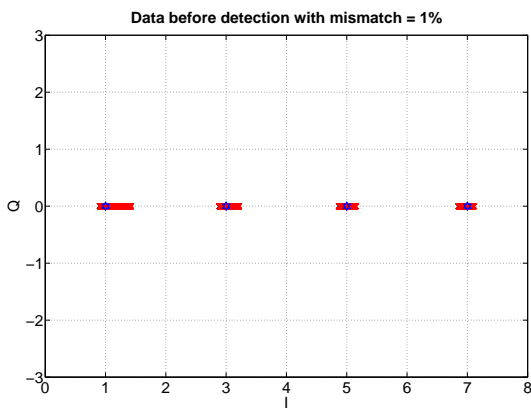
Figure 4: Scatter plot with 1.5% mismatch
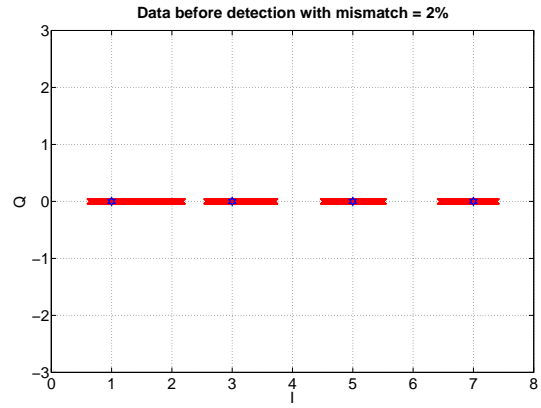

Figure 3: Scatter plot with 1% mismatch

Figure 5: Scatter plot with 2% mismatch

- Scatter Plot

- Signal-to-Distortion Ratio (SDR)

- Bit Error Rate (BER)

- Error Vector Magnitude (EVM)

The analysis has been worked out by varying the mismatch between the chromatic dispersion value used to compute the pre-compensation filter and that of the actual chromatic dispersion introduced by the channel for different values of signal-to-noise ratio (SNR). The SNR is defined as

$$SNR = \frac{P_a}{\sigma_n^2}, \qquad (6)$$

where

$$P_a = \frac{1}{|\mathcal{A}|} \sum_{i=0}^{|\mathcal{A}|-1} a_i^2 = 21. \qquad (7)$$

is the average power of $\{a_k\}$, being $\mathcal{A}$ the cardinality of the set $\mathcal{A}$.

In what follows, the mismatch m is expressed as percentage of the product DL so that the resulting chromatic dispersion transfer function is

$$H_P(f) = \exp(\frac{-j\pi DL(1+m)\lambda^2}{c}f^2). \qquad (8)$$

where $0 < m < 1$ is the percentage of mismatch.

3.1 Scatter Plot

The scatter plot is a graphic tool that allows for visualizing how received symbols spread around the ideal constellation points. The larger is the distortion, the larger is the dispersion around the correct constellation point. Figures 2, 3, 4, and 5 show how the symbols at the input of the threshold detector spread around the corresponding reference points for increasing values of the percentage of mismatch. Note that in the following, both positive and negative values of m will be considered since, due to symmetry in the frequency response of the chromatic dispersion, they give exactly the same result for the same absolute value of percentage.
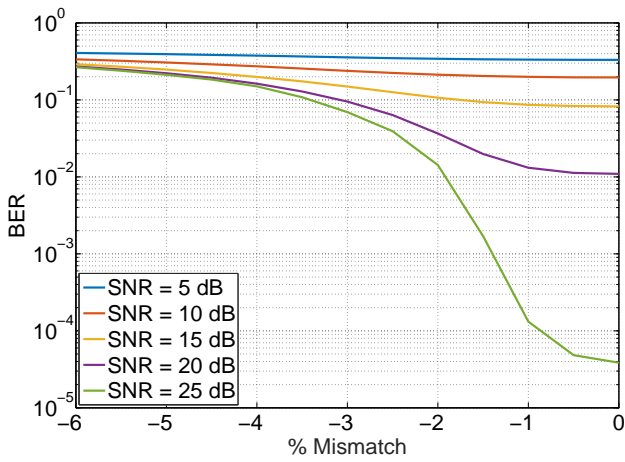
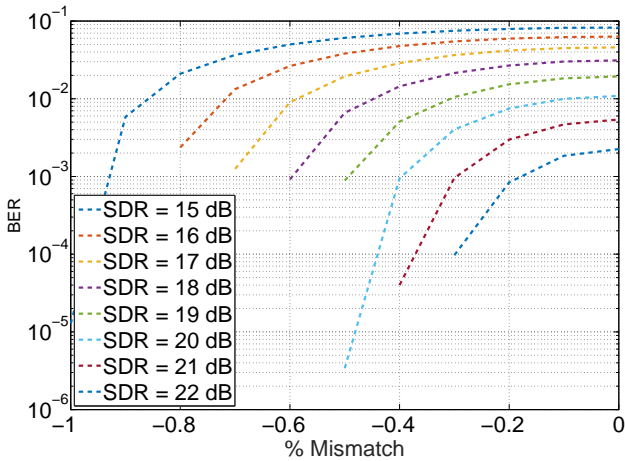Figure 6: BER versus % of mismatch for different values of SNR.

Figure 7: BER versus % of mismatch for different SDR values.

It is possible to see that the symbols with smaller values are the ones that are more affected by the chromatic dispersion, because they suffer the impact of the higher symbols spreading in time. So the scatter plot is more dispersed around amplitude level 1 than around amplitude level 7.

3.2 Signal-to-Distortion Ratio

The SDR measured at the input of the photo-detector is defined as the ratio between the power of the desired signal and the power of the total distortion, that is the sum of noise and ISI, and is given by

$$SDR = \frac{P_a}{P_{ISI} + \text{SNR}^{-1}P_a} \qquad (9)$$

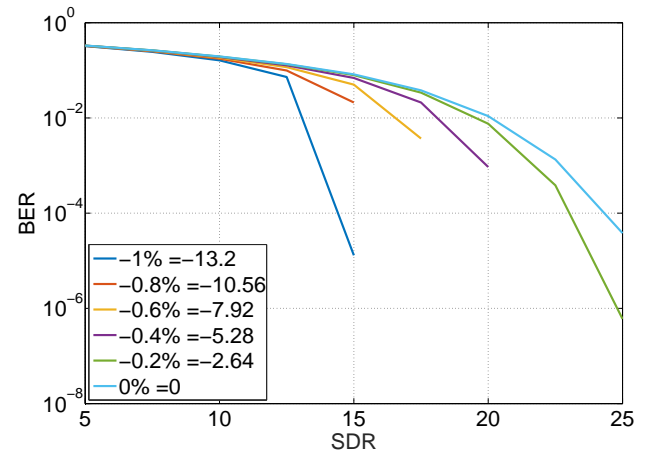The power of the ISI term is calculated as

Figure 8: BER versus SDR for different values of % mismatches.

$$P_{ISI} = P_a \sum_k |1 - h_m(k)|^2 . \qquad (10)$$

3.3 Bit Error Rate

In the simulation, the BER performance has been evaluated by comparing the transmitted bit sequence with that estimated produced at the output of the demodulator. Evaluation of BER has been done by varying the SNR level and the mismatch percentage, by keeping fixed the other parameters. In Fig. 6 each individual curve is parameterized with a fixed SNR. From the Figure it is possible to appreciate how the performance gets worse as the percentage of the mismatch increases.

Figure 7 reports individual BER curves versus the mismatch for a fixed SDR, that is, by changing the relative powers of noise and ISI to have a constant SDR in (9). It can be observed that at fixed measured SDR the BER decreases with the increase of the mismatch percentage and, therefore, it is in some way possible to evaluate the entity of mismatch by jointly measuring BER and SDR.

In Fig. 8 each individual curve has a constant mismatch. From Figs. 7 and 8 it can be observed that when the total power of the distortion is dominated by the ISI, that actually is not Gaussian, there are less errors than what expected from the Gaussian approximation.

3.4 Error Vector Magnitude

The data-aided Error Vector Magnitude (EVM) computation is given by [10, 11]

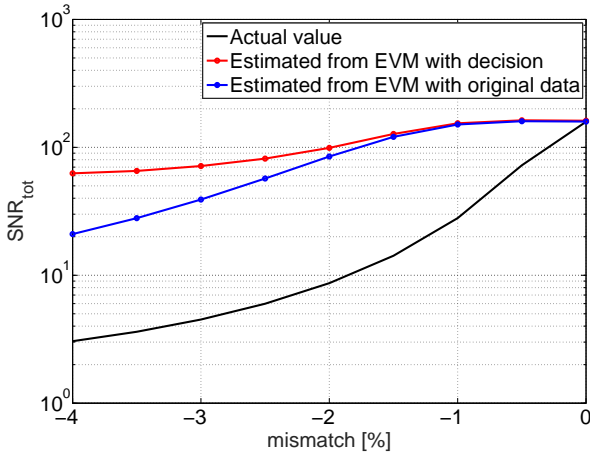$$EVM = \sqrt{\frac{1/K \sum_{k=1}^{K} |r_k - a_k|^2}{P_a}} \qquad (11)$$

Figure 9: Comparison between actual SNR_{tot} and the estimated one.

where a_k is the ideal transmitted value that corresponds to r_k, P_a is the average symbol power evaluated in (7) and K is the number of samples used for averaging.

The EVM is calculated before the threshold detector at the output of the photo-detector and used to compute the BER. EVM is an indicator of how much the received signal deviates from the points of the original constellation. It is linked to the total SNR_{tot} observed at the input of the threshold detector as

$$EVM = \sqrt{\frac{1}{\text{SNR}_{tot}}}. \qquad (12)$$

Figure 9 shows the SNR_{tot} estimated by the EVM when the latter is evaluated both by making the difference between the received symbols and the original transmitted data (data-aided EVM, defined in (11)) and by using decisions $\hat{a}_k$ in (11) in place of the actual data (non data-aided EVM) for the case where SNR=22 dB. Clearly, using decisions with small SNR_{tot}, the EVM is underestimated because in case of error, the decision device chooses the nearest symbol and not the correct one.

The BER is estimated by substituting the SNR_{tot} obtained from (12) using the estimated EVM in analytical expression that gives the bit error probability for the considered PAM-4 modulation scheme as

$$P_b(e) \approx \frac{2(M-1)}{M \log_2 M} Q\left(\sqrt{\frac{\text{SNR}_{tot}}{P_a}}\right) \qquad (13)$$

where $Q(\cdot)$ is the Q-function used when the distortion is Gaussian distortion, hence under the Gaussian approximation of ISI.

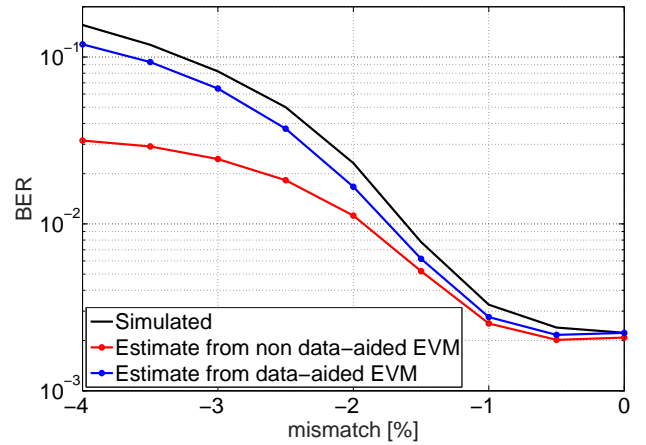Figure 10 reports the BER evaluated using the estimated EVM both for the data-aided and the non

Figure 10: BER versus % of mismatch for SNR=22 dB obtained from Monte Carlo simulation, data-aided EVM and non data-aided EVM.

data-aided case. As it can be observed from the Figure, while the BER obtained using the data-aided estimated EVM provides a good estimate of the real BER obtained by Monte Carlo simulation for all the values of mismatch, the BER obtained using estimated EVM with decisions provides a good approximation only for mismatch values below -2%.

4 Conclusion

The main advantage of intensity modulated PAM-4 with direct detection (IM-DD PAM-4) is that of allowing for a dramatically reduction of the cost of the receiver. As such, it is a solution that is currently object of many investigations especially in short-reach optical communication systems. However, linear distortion effects introduced by the channel could limit its applicability. In this paper we consider the effect of chromatic dispersion and, in order to compensate for it, we propose to introduce a pre-compensation filter in the transmitter. Since the exact value of the dispersion is not known exactly, we evaluate the sensitivity of the performance IM-DD PAM-4 to mismatches between the value of dispersion used in the pre-compensation filter and the actual one of the channel by using different quantitative Figure of merits. Simulation results show that, among the considered methods, error vector magnitude is able to provide a good estimate of the performance degradation in terms of bit error rate for a given value of the mismatch.

References:

[1] P. Little (2014, June), Who's afraid of the big, bad DSP? [Online]. Available: `http://www.ethernetalliance.org`

[2] K. Zhong *et al.*, Experimental study of PAM-4, CAP-16, and DMT for 100 Gb/s short reach optical transmission systems, *Opt. Express* 23, 2015, pp. 1176–1189.

[3] B. Xu, L. Zhang and K. Qiu, Memory-based pulse amplitude modulation for short-reach fiber communications with intensity modulation and direct detection, *Opt. Express* 24, 2016, pp. 11876–11884.

[4] L. Barletta, F. Bergamelli, M. Magarini, N. Carapellese and A. Spalvieri, Pilot-aided trellis-based demodulation, *IEEE Photon. Technol. Lett.* 25, 2013, pp. 1234–1237.

[5] L. Barletta, M. Magarini and A. Spalvieri, Staged demodulation and decoding, *Opt. Express* 20, 2012, pp. 23728–23734.

[6] J. von Hoyningen–Heune, OFDM for Optical Access, *Optical Fiber Communication Conference (OFC)*, 2015.

[7] C. Xie *et al.*, Single-VCSEL 100-Gb/s short reach system using discrete multi-tone modulation and direct detection, *Optical Fiber Communication Conference* (OFC), 2015.

[8] M. Magarini, L. Barletta and A. Spalvieri, Efficient computation of the feedback filter for the hybrid decision feedback equalizer in highly dispersive channels, *IEEE Trans. Wireless Commun.* 11, 2012, pp. 2245–2253.

[9] D. Che, Q. Hu and W. Shieh, Linearization of direct detection optical channels using self-coherent subsystems, *J. Lightw. Technol.* 34, 2016, pp. 516–524.

[10] Z. Dong, F. N. Khan, Q. Sui, K. Zhong, C. Lu, A. Pak Tao Lau, Optical performance monitoring: a review of current and future technologies, *J. Lightw. Technol.* 34, 2016, pp. 525–543.

[11] R. Schmogrow *et al.*, Error vector magnitude as a performance measure for advanced modulation formats, *IEEE Photon. Technol. Lett.* 24, 2012, pp. 1041–1135.